Efficient backward-propagation using wavelet-based filtering for fiber backward-propagation

Gilad Goldfarb and Guifang Li

College of Optics & Photonics/CREOL&FPCE, University of Central Florida
4000 Central Florida Blvd., Orlando, FL 32816-2700
gilad@creol.ucf.edu, li@creol.ucf.edu

Abstract: With the goal of reducing the number of operations required for digital backward-propagation used for fiber impairment compensation, wavelet-based filtering is presented. The wavelet-based design relies on signal decomposition using time-limited basis functions and hence is more compatible with the dispersion operator, which is also time-limited. This is in comparison with inverse-Fourier filter design which by definition is not time-limited due to the use of harmonic basis functions for signal decomposition. Artificial, after-the-fact windowing may be employed in this case; however only a limited amount of saving in the number of operations can be achieved, compared to the wavelets-base filter design. Wavelet-based filter design procedure and numerical simulations which validate this approach are presented in this paper.

OCIS codes: (060.1660) Coherent communications; (060.4370) Nonlinear optics, fibers.

References and links

1. A. D. Ellis and F. C. G. Gunning, "Spectral density enhancement using coherent WDM," IEEE Photon. Technol. Lett. **17**, 504-506 (2005).
2. G. Goldfarb, G. Li, and M. G. Taylor, "Orthogonal Wavelength-Division Multiplexing Using Coherent Detection," IEEE Photon. Technol. Lett. **19**, 2015-2017 (2007).
3. S. J. Savory, G. Gavioli, R. I. Killey, and P. Bayvel, "Electronic compensation of chromatic dispersion using a digital coherent receiver," Opt. Express **15**, 2120-2126 (2007).
4. G. P. Agrawal, *Nonlinear Fiber Optics*, 4th. ed., (Academic Press, 2007).
5. A. Yariv, D. Fekete, and D. M. Pepper, "Compensation for channel dispersion by nonlinear optical phase conjugation," Opt. Lett. **4**, 52–54 (1979).
6. R. A. Fisher, B. R. Suydam, and D. Yevick, "Optical phase conjugation for time-domain undoing of dispersive self-phase-modulation effects," Opt. Lett. **12**, 611-613 (1983).
7. C. Pare, A. Villeneuve, P. A. Belanger, and N. J. Doran, "Compensating for dispersion and the nonlinear Kerr effect without phase conjugation," Opt. Lett. **21**, 459-461 (1996).
8. R.-J. Essiambre, P. J. Winzer, X. Q. Wang, W. Lee, C. A. White, and E. C. Burrows, "Electronic predistortion and fiber nonlinearity," IEEE Photon. Technol. Lett. **18**, 1804-1806 (2006).
9. R. I. Killey, P. M. Watts, V. Mikhailov, M. Glick, and P. Bayvel, "Electronic dispersion compensation by signal predistortion using digital Processing and a dual-drive Mach-Zehnder Modulator," IEEE Photon. Technol. Lett. **17**, 714-716 (2005).
10. K. Roberts, L. Chuandong, L. Strawczynski, M. O'Sullivan, and I. Hardcastle, "Electronic precompensation of optical nonlinearity," IEEE Photon. Technol. Lett. **18**, 403-405 (2006).
11. E. Yamazaki, F. Inuzuka, K. Yonenaga, A. Takada, and M. Koga, "Compensation of Interchannel Crosstalk Induced by Optical Fiber Nonlinearity in Carrier Phase-Locked WDM System," IEEE Photon. Technol. Lett. **19**, 9-11 (2007).
12. L. B. Y. Du and A. J. Lowery, "Fiber nonlinearity precompensation for long-haul links using direct-detection optical OFDM," Opt. Express **16**, 6209-6215 (2008).
13. X. Li, X. Chen, G. Goldfarb, E. Mateo, I. Kim, F. Yaman, and G. Li, "Electronic post-compensation of WDM transmission impairments using coherent detection and digital signal processing," Opt. Express **16**, 880-888 (2008).
14. G. Goldfarb, M. G. Taylor, and G. Li, "Experimental Demonstration of Fiber Impairment Compensation Using the Split-Step Finite-Impulse-Response Filtering Method," IEEE Photon. Technol. Lett. **20**, 1887-1889 (2008).
15. G. Goldfarb and G. Li, "Demonstration of fibre impairment compensation using split-step infinite-impulse-response filtering method," Electron. Lett. **44**, 814-816 (2008).
16. X. Li, C. Xingzhong, and M. Qasmi, "A broad-band digital filtering approach for time-domain Simulation of pulse propagation in optical fiber," J. Lightwave Technol. **23**, 864-875 (2005).

#107052 - $15.00 USD Received 2 Feb 2009; revised 4 Apr 2009; accepted 6 Apr 2009; published 12 May 2009

17. T. Kremp and W. Freude, "Fast split-step wavelet collocation method for WDM system parameter optimization," J. Lightwave Technol. **23**, 1491-1502 (2005).
18. G. Beylkin, "On the Representation of Operators in Bases of Compactly Supported Wavelets," SIAM J. on Numerical Analysis **29**, 1716-1740 (1992).

1. Introduction

One of the benefits associated with coherent optical transmission systems is the possibility to obtain higher spectral-efficiency compared to direct or differential detection. High spectral-efficiency may be achieved in several ways: tight channel spacing (e.g., [1, 2]), advanced modulation formats (e.g., M-ary phase shift keying or quadrature-amplitude modulation), polarization multiplexing (e.g., [3]) or a combination of these techniques. The increase in spectral-efficiency is usually accompanied by higher sensitivity to degrading fiber propagation effects which stem from the interaction between dispersion and nonlinearity. Mitigation of nonlinear effects can be achieved by using dispersion-managed systems [4], but this solution introduces added noise and is quite rigid.

Alternatively, digital signal processing (DSP) may be used to achieve backward-propagation, as explained in the following. The concept of backward-propagating an optical signal to mitigate transmission effect stems from Yariv *et al.* which in 1979 suggested the use of phase-conjugation for dispersion compensation [5]. Fisher *et al.* extended this notion in 1983 to compensate for both dispersion and Kerr nonlinearity [6]. The use of a medium with negative nonlinear index (e.g., semiconductors) to reverse the effects of transmission without phase conjugation was suggested in [7]. An examination of the nonlinear Schrödinger equation (NLSE), which governs the evolution of optical signal propagation in fiber with Kerr nonlinearity, reveals that all these techniques amount to reversing the fiber parameters (either dispersion, nonlinear index, or both). This is mathematically equivalent to reversing the spatial variable sign in the NLSE and hence the technique is referred to as backward-propagation.

Electronic pre-distortion of the signal was considered in [8-10] and experimental demonstrations using dispersion-managed links with subsequent nonlinear phase fluctuation mitigation (lumped post-compensation) using DSP are presented in [11, 12]. Post-compensation via backward-propagation takes into account all deterministic effects in fiber, allows the use of conventional transmitter architecture and offers flexibility through adaptive processing. Numerical simulations of a wavelength-division multiplexing (WDM) system with post-compensation of both linear and nonlinear effects were presented in [13]. An experimental demonstration of the feasibility of receiver-side backward-propagation in an orthogonal-WDM system environment soon followed [14].

Efficient real-time implementation of any DSP algorithm in a communication system context is crucial in order to reduce transmission latency and power consumption. Finite impulse response (FIR) filtering is highly compatible with real-time DSP implementation, as compared to other filtering techniques. It does, however, suffer from limited efficiency. In this paper, the authors suggest a wavelet-based FIR filter design used for backward-propagation, which is shown to achieve higher efficiency compared to alternative filter design procedures. In section 2 the method of achieving digital backward-propagation is presented. Section 3 explains the wavelet-based design procedure and in section 4 simulation results validating the efficiency of this approach are presented. Conclusions are presented in section 5.

2. Backward-propagation using the split-step method

Backward propagation is achieved using DSP after coherent detection (with which complete information of the received complex-field is preserved). After sampling at the appropriate rate, the received signal is backward-propagated by solving the NLSE (for a single polarization) with the spatial variable negated:

$$\frac{\partial A}{\partial(-z)} = (\hat{D} + \hat{N})A \tag{1}$$

#107052 - $15.00 USD Received 2 Feb 2009; revised 4 Apr 2009; accepted 6 Apr 2009; published 12 May 2009

where A is the complex electric field, $\hat{D}$ is the linear operator accounting for dispersion as well as fiber loss and $\hat{N}$ is the nonlinear operator, which takes Kerr nonlinearity into account. These operators are given by:

$$\hat{D} = -j\frac{\beta_2}{2}\frac{\partial^2}{\partial t^2} + \frac{\beta_3}{6}\frac{\partial^3}{\partial t^3} - \frac{\alpha}{2} \tag{2a}$$

$$\hat{N} = j\gamma\left|A\right|^2 \tag{2b}$$

where α, β_2, β_3 and γ are the attenuation factor, first- and second-order group-velocity dispersion and the nonlinearity parameter, respectively. The symmetric-SSM is used to solve Eq. (1) by dividing each fiber span into N_{steps} steps, each of z_{step} length. The total propagation length for N_{spans} is $z_{fiber} = N_{spans} z_{span}$ where $z_{span} = N_{steps} z_{step}$. At each step the corresponding linear [Eq. (2a)] and nonlinear [Eq. (2b)] compensation is performed. Note that using the symmetric-SSM, the linear operator is compensated first using half the step size. $N_{steps} - 1$ sequential nonlinear and linear full-step compensation operations follow and the last step consists of a single nonlinear (full-step) and linear (half-step) operations. This simple modification to the asymmetric-SSM achieves higher accuracy for a given step size [4]. Fiber loss is accounted for at each step, while amplification (required after each span to compensate for fiber loss of $L = 1/G = \exp\left\{-\alpha z_{span}\right\}$) is reversed before each span. Backward-propagation for a single span using the symmetric-SSM is illustrated in Fig. 1.

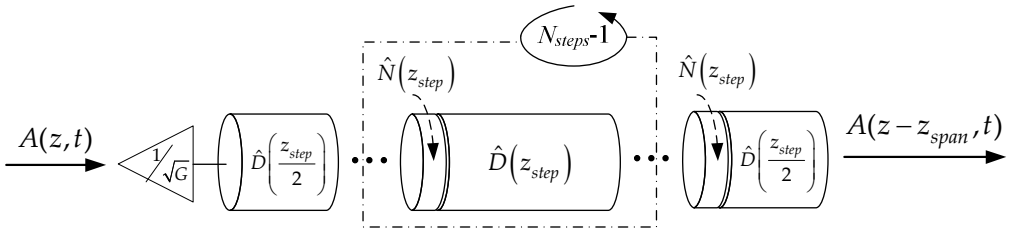

Fig. 1. Single span backward-propagation using the symmetric-SSM.

Accurate backward-propagation of a multichannel optical signal requires the SSM step size to be small enough so that the assumption that dispersion and nonlinearity act independently is valid [4]. A major difficulty in implementing this technique is the high computational load associated with the dispersion operator. This operator can be implemented in the frequency-domain (via fast Fourier transform, FFT) or in the time-domain using filters. For real-time compatible implementation, FIR filtering is a practical choice as it does not require block-processing (as opposed to FFT implementation). Moreover, FIR filtering does not require a feedback path, as opposed to the use of infinite-impulse response filtering, which was shown to be highly efficient [15], but is hard to implement in real-time.

The FIR filter coefficients may be obtained by an inverse-Fourier transform (IFT) of the dispersion frequency response of each step, given in Eq. (2a). This makes the filter length identical to the IFT length, which should be made long enough to achieve high accuracy of the SSM. To reduce the SSM computational load, time-domain windowing of the dispersion compensating FIR filter may be considered; e.g., using Tukey windowing [16]. The window width should be approximately on the order of the time-frame related to the dispersion-induced pulse spreading over a single step, given by:

$$N_{lin} = \Delta\lambda D z_{step} / T_s \tag{3}$$

#107052 - $15.00 USD Received 2 Feb 2009; revised 4 Apr 2009; accepted 6 Apr 2009; published 12 May 2009

where $\Delta\lambda, D$ and T_s are the optical bandwidth, dispersion parameter (in ps/km/nm) and the sampling interval, respectively. There is however, a fundamental issue associated with windowing of the FIR filter: the loss of the all-pass property of the dispersion operator. The all-pass property means that the transfer function of the filter used for dispersion compensation, $H_f(\omega)$, should be lossless, i.e. $|H_f(\omega)| = 1, \forall \omega$. As multiple steps of dispersion compensation are required by the SSM, the accumulated error from the windowing of the FIR filter becomes significant and the ultimate quality of the backward-propagated signal is deteriorated. IFT-based design of the FIR dispersion compensation filter is sub-optimal since the Fourier transform relies on a harmonic decomposition basis which is not time-limited and windowing is hence required. Wavelet-based filter design of the dispersion operator is based on time-limited decomposition. This approach is shown to achieve accurate back-propagation while reducing the number of operations required for the linear operator, as shown in the following.

3. Wavelet-based FIR filter design

Wavelet-based FIR filter design makes use of compact-support decomposition functions. Compact support functions are only non-zero on a finite interval, as opposed to the harmonic basis. As suggested in [17], a possible choice for the decomposition basis is the Deslaurier-Duruc interpolating scaling function $\phi(t)$. The function's support is determined by a single (odd) parameter s. The compact-support property is stated as: $\phi(t) \equiv 0, \forall |t| > sT_s$. The interpolating scaling function is defined by a filter whose coefficients are given by [17]:

$$h_{2k} = \delta_k \tag{4a}$$

$$h_{2k+1} = h_{-(2k+1)} = \frac{(-1)^{\frac{s+1}{2}-k} \prod_{q=0}^{s} \left(q - \frac{s}{2}\right)}{\left(\frac{s-1}{2}-k\right)!\left(\frac{s+1}{2}+k\right)!\left(k+\frac{1}{2}\right)} \tag{4b}$$

where δ_k is the Kroneker delta function. The compact support of $\phi(t)$ dictates that $h_k \equiv 0, \forall |k| > s$. The parameter s is used to match the dispersion compensating filter length to the required dispersion-induced pulse spreading time-frame [from (Eq. 3)]. Two interpolating functions with $s = 3, 7$ are shown in Fig. 2.

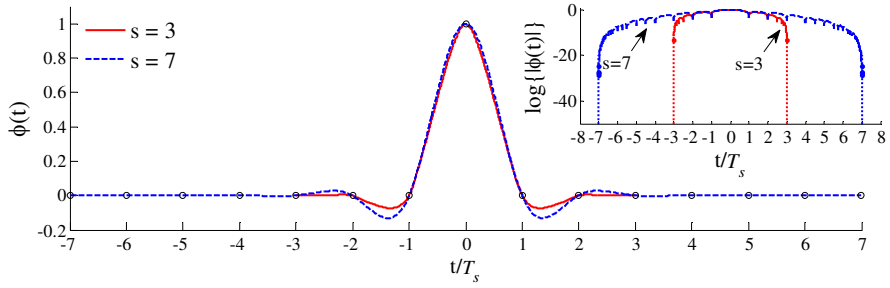

Fig. 2. $\phi(t)$ with $s = 3, 7$. Inset: $\log\{|\phi(t)|\}$.

The compact-support of $\phi(t)$ is clearly seen in Fig. 2 (inset) with $\phi(t)$ being identical to zero for times beyond $|t| > sT_s$.

#107052 - $15.00 USD Received 2 Feb 2009; revised 4 Apr 2009; accepted 6 Apr 2009; published 12 May 2009

The linear operator requires finding the second and third order derivatives of the time-shifted interpolation function $\phi_m(t) = \phi(t - t_m)$, where t_m are the sampling instances). To achieve this, vectors $\overrightarrow{D^{(\mu)}}$ of $2s-1$ elements each are found by solving the linear set of equations defined in [18]. Keeping the same notation as in [17] ($\mu = 2,3$ for the second and third order derivative, respectively), the following set of equations is to be solved:

$$\sum_{k=-(s+1)/2}^{(s-1)/2} h_{2k+1} D^{(\mu)}_{2(k+n)+1} - 2^{-\mu} D^{(\mu)}_n + D^{(\mu)}_{2n} = 0 \tag{5a}$$

$$\sum_{n=1-s}^{s-1} n^{\mu} D^{(\mu)}_n = \mu! \tag{5b}$$

where n is an integer and Eq. (5b) is used for normalization. The compact support limits the number of nonzero elements of $\overrightarrow{D^{(\mu)}}$ so that $D_n \equiv 0, \forall |n| \geq s$. The elements of $\overrightarrow{D^{(\mu)}}$ are symmetric for $\mu = 2$ and anti-symmetric for $\mu = 3$, such that: $D^{(\mu)}_{-k} = (-1)^{\mu} D^{(\mu)}_k$, so that there are s equations required to obtain $\overrightarrow{D^{(\mu)}}$. The Wavelet-based FIR filter used for dispersion compensation is given by the following equation, where an extension from [17] to introduce second-order group-velocity dispersion is included:

$$\overrightarrow{h_f} = IFFT\left\{\exp\left\{\left\{FFT\left[\frac{1}{2T_s^2}\left(-j\beta_2 \overrightarrow{D^{(2)}} + \frac{\beta_3 \overrightarrow{D^{(3)}}}{3T_s}\right)\right] + \frac{\alpha}{2}\right\} z_{step}\right\}\right\}. \tag{6}$$

In order for $\overrightarrow{h_f}$ to obtain high accuracy, $\overrightarrow{D^{(2,3)}}$ are zero-padded (before the Fourier transform) so that the impulse response is longer than the limit given by Eq. (3). $\overrightarrow{h_f}$ is then truncated to allow savings in number of operations by setting all the coefficients that result in $\log\left\{\left|\overrightarrow{h_f}\right|\right\} < \varepsilon$ to zero. ε may be scanned to obtain a value which allows good performance while minimizing the number of non-zero $\overrightarrow{h_f}$ coefficients.

4. Numerical simulation

To investigate the benefit of wavelet-based FIR filter design, simulation of a 9 channel WDM system was performed. Quadrature phase-shift keying (QPSK) modulation at 10GBaud, with 20GHz channel spacing was employed. The simulation sampling rate used was set to 320GHz ($T_s = 3.125\,ps$) and pseudo-random bit sequence of order 23 was used. The optical signal was launched into 48 spans of 100km non-zero dispersion shifted fiber (NZ-DSF). The fiber parameters are $\alpha = 0.2dB/km$, $D = 4\,ps/km/nm$, $D_s = 0.045\,ps/km/nm^2$ and $\gamma = 1.46/W/km$, where D_s is the dispersion slope. The loss in each span was compensated using an optical amplifier with noise figure $N_F = 5$.

Verification of the benefit of using backward-propagation as compared to linear (dispersion) compensation only is seen in Fig. 3. The total launching power is scanned to demonstrate the ability to achieve better performance using backward-propagation, compared to linear compensation only. Backward-propagation is implemented as discussed in Section 2, with frequency domain dispersion compensation (SSM/FFT). Using frequency domain

#107052 - $15.00 USD Received 2 Feb 2009; revised 4 Apr 2009; accepted 6 Apr 2009; published 12 May 2009

compensation no time-domain effects (such as FIR windowing) deteriorate the performance. SSM/FFT is hence used as the benchmark for backward-propagation performance. Also included is the performance limit when all the fiber parameters except loss are set to zero; in this case, only amplifier noise and linear interference affect the performance. The phase standard-deviation (Phase-STD) serves as a metric for the performance since phase shift keying is considered in this numerical study. From Fig. 3, the benefit of using backward-propagation is clear as the optimal launching power is increased and the performance improved. The optimum total launching power is found to be $5dBm$ and an SSM step size of $2km$ was determined to achieve close to zero penalty performance, compared to smaller step sizes. These values will be used in the following analysis.

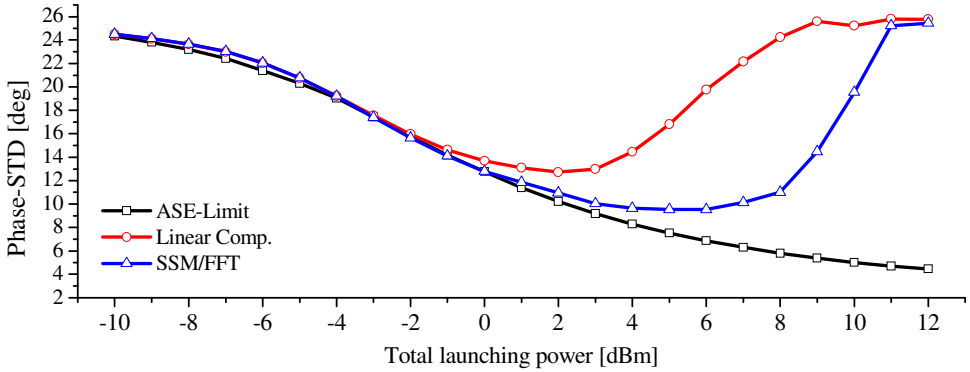

Fig. 3. ASE-Limit (no dipersion or nonlinear effects), linear compensation and backward-propagation performance vs. total launching power.

A comparison of three FIR filters using IFT, IFT with Tukey windowing (both in frequency and time, as in [16]) and wavelet-based design is seen in Fig. 4.

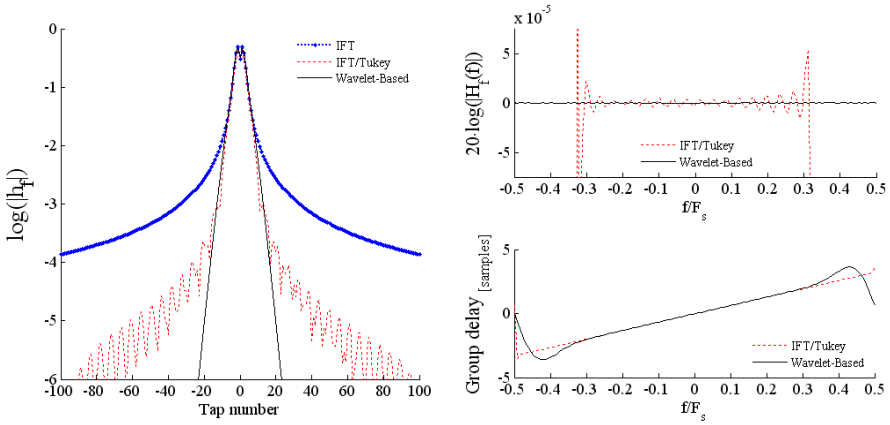

Fig. 4. Impulse response of dispersion compensation FIR filter with IFT, IFT/Tukey and Wavelets-based designs (left), magnitude response (top right) and group-delay response (bottom right).

On the left, the time-domain magnitude, namely the impulse response is plotted on a logarithmic scale for clarity. The plot reveals the slow decay of the IFT filter; Tukey windowing limits the extent (and hence the number of operations required for filtering) of the IFT-based filter. Wavelets-based design achieves tighter windowing limits due to the compact-support of the decomposition function it is based upon. Moreover, observing the magnitude response comparison between IFT/Tukey and wavelets-based designs (Fig. 4, top right) shows that the all-pass characteristic of the wavelet-based filter is preserved much better

#107052 - $15.00 USD Received 2 Feb 2009; revised 4 Apr 2009; accepted 6 Apr 2009; published 12 May 2009

than with the IFT/Tukey design. Although the IFT/Tukey filter group-delay (Fig. 4, bottom right) is more accurate (namely, closer to the required linear group-delay response) at the band edges than the wavelet-based filter, loss of the all-pass feature combined with multiple linear-compensation operations required when employing the SSM is a significantly more severe issue.

The number of FIR filter coefficients for IFT/Tukey was scanned by varying the Tukey window ratios of both frequency and time windows used. For the wavelets-based filter, the parameter s was scanned increasingly by taking values starting from N_{lin} given in Eq. (3) with the parameter $\varepsilon = -12$ to find the smallest limit on s which allows a wide enough window to include the effect of dispersion-induced pulse spreading. A value of $s = 27$ was found to be sufficient. Truncation of the wavelet-based FIR filter by increasing the value of ε minimizes the number of operations required for the linear operator in the SSM. A performance comparison of the two filter designs is shown in Fig. 5. The performance limit of the SSM achieved with the linear operator implemented in the frequency domain (FFT) is also shown.

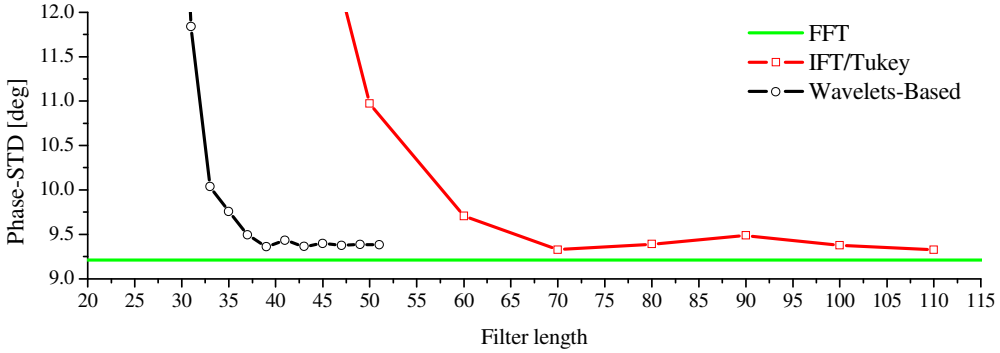

Fig. 5. Performance comparison of IFT/Tukey and wavelets-based FIR filter design vs. filter length.

From Fig. 5, it is observed that the wavelets-based FIR filtering approach achieves equivalent performance as the IFT/Tukey design (both being close to the frequency-domain linear compensation implementation). The wavelet-based filter achieves this performance using 39 taps, as opposed to 70 taps for the IFT/Tukey design. The number of filter taps required for the SSM linear operator is hence reduced by a factor of approximately 1.8, validating the wavelet-based approach to dispersion-compensation FIR filter design. Although the wavelets-based is more efficient than IFT-based ones, the implementation of backward-propagation leads to a larger computational load and latency, compared to lumped linear compensation only. The backward-propagation scheme's additional computational load and latency should be taken into account as an engineering trade-off with its superior performance, compared to linear compensation only.

5. Conclusions

In this contribution, the authors suggest an alternative approach to FIR filter design used for digital backward-propagation of an optical signal propagated in a nonlinear fiber. FIR filtering is highly compatible with real-time implementation, yet suffers from a large computational load requirement. The compact support of the wavelet decomposition basis function leads to a rapid decay of the FIR filter coefficients, as opposed to inverse-FT design. This rapid decay allows truncation of filter coefficients without severely affecting the all-pass property of the FIR filter used. Simulation was conducted for a WDM system with 9 channels, each QPSK modulated at $10GBaud$, with $20GHz$ channels spacing. The optical signal was propagated in 48 spans of $100km$ NZ-DSF and the SSM was used for backward propagation. The wavelet-based design achieves equivalent performance as IFT-based design with Tukey windowing, with a reduction of approximately 1.8 in filter length for the WDM configuration presented.

#107052 - $15.00 USD Received 2 Feb 2009; revised 4 Apr 2009; accepted 6 Apr 2009; published 12 May 2009